



Copyright Statement

The digital copy of this thesis is protected by the Copyright Act 1994 (New Zealand). This thesis may be consulted by you, provided you comply with the provisions of the Act and the following conditions of use:

- Any use you make of these documents or images must be for research or private study purposes only, and you may not make them available to any other person.
- Authors control the copyright of their thesis. You will recognise the author's right to be identified as the author of this thesis, and due acknowledgement will be made to the author where appropriate.
- You will obtain the author's permission before publishing any material from their thesis.

To request permissions please use the Feedback form on our webpage.

<http://researchspace.auckland.ac.nz/feedback>

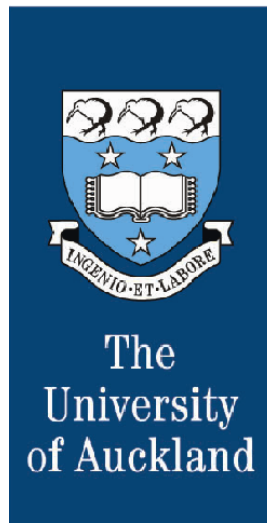
General copyright and disclaimer

In addition to the above conditions, authors give their consent for the digital copy of their work to be used subject to the conditions specified on the Library

[Thesis Consent Form](#)

**SIMULATION OF COMPLEX MULTI-
PHASE, MULTI-COMPONENT, REACTING
FLOWS IN POROUS MEDIA**

Sadiq J. Zarrouk



A thesis submitted in partial fulfillment
of the requirements for the degree of
Doctor of Philosophy
in
Engineering Science

The University of Auckland
June 2004

Abstract

In this study we are concerned with the modelling of multi-component, multi-phase chemically reacting flows in porous media, with particular application to the spontaneous combustion of coal and the extraction of coalbed methane.

These two related problems involve complex multiphase, multi-component flow in a porous medium. Chemical reactions, adsorption, gaseous diffusion and changes in porosity and permeability are important in one or both of these problems. These matters are discussed in general in the first few chapters of the thesis.

Several models for the spontaneous combustion of coal that include the effect of a diminishing reaction rate are investigated and a new formulation in the form of a generic power law model is introduced.

A numerical module for modelling the spontaneous combustion of coal is described, based on the TOUGH2 code. A new equation of state (EOS) module is developed including realistic physical properties for all gases involved. The modified version of TOUGH2 is used for modelling the adiabatic method for testing the reactivity of coal samples. The results agree very well with experimental measurements for coal samples from different mines in New Zealand and Australia.

Moisture effect on the reaction rate was then introduced to TOUGH2 using a new two-phase EOS module with water and air broken into its main components (Nitrogen, Oxygen, Carbon dioxide and Argon).

Finally the production of methane from low rank coalbeds is investigated. A new EOS for mixture of water and methane is developed and incorporated into the TOUGH2 code to produce a new and versatile coalbed methane simulator. It is validated by running

some simple test problems and comparing results with those obtained with the commercial COMET simulator.

Acknowledgements

- First of all I would like to express my deepest gratitude to Professor Mike O’Sullivan: my research supervisor, for being so much patient with me during my work and for his fruitful advice and guidance as well as the financial help without which I could not have pursued my work.
- I also appreciate very much the efforts of Associate Professor Arnold Watson along with all the staff of the Geothermal Institute for their valuable help, advice and financial assistance.
- A special thanks to Associate Professor Mohamed Farid of the department of chemical and materials engineering, University of Auckland for his kind advice.
- Many sincere thanks to Dr. John St George of the department of civil and environmental engineering, University of Auckland for the rewarding discussions and for providing the data for the New Zealand coal.
- I would also like to express my gratitude to Mr. Shane Wright and Dr. Basil B. Beamish, University of Queensland, Brisbane, for the test work and for their kind permission to release unpublished data.
- Many thanks to Callide Coal fields Pty Ltd. (Australia) for supplying the fresh face coal samples.
- I am much obliged to all my fellow postgraduate and office-mates: Isabel, Mathew, Warren, Juliet and Adrian for their assistance, fruitful discussions and most of all for deciphering Mike’s hand writing.
- My gratitude to all the staff of the engineering library for providing the necessary manuscripts for the extensive review.

To My Homeland Iraq

Contents

<i>Abstract</i>	<i>ii</i>
<i>Acknowledgments</i>	<i>iv</i>
<i>Dedication</i>	<i>v</i>
<i>Contents</i>	<i>vi</i>
<i>List of Figures</i>	<i>xii</i>
<i>List of Tables</i>	<i>xix</i>
<i>Nomenclature</i>	<i>xxi</i>

CHAPTER 1: CHEMICAL REACTION IN POROUS MEDIA 1

1.1	INTRODUCTION	1
1.2	CHEMICAL REACTIONS	3
1.2.1	<i>Chemical kinetics</i>	4
1.2.2	<i>Equilibrium models</i>	10
1.2.3	<i>Mixed equilibrium-kinetic system</i>	13
1.3	CHEMISORPTION (CHEMICAL ADSORPTION).....	17
1.4	MICROBIOLOGICAL REACTIVE MODELLING.....	19
1.5	MODELLING CHEMICAL REACTION AS ODE'S.....	21
1.6	CONCLUSIONS.....	24

CHAPTER 2: THE EFFECT OF CHEMICAL REACTIONS ON THE TRANSPORT PROPERTIES OF POROUS MEDIA .. 26

2.1	INTRODUCTION	26
2.2	CHANGES IN POROSITY DUE TO CHEMICAL REACTION.....	30
2.2.1	<i>Continuum model</i>	30
2.2.2	<i>Spherical grain model</i>	33
2.2.3	<i>Cubic grain model</i>	34
2.3	CHANGES IN PERMEABILITY DUE TO CHEMICAL REACTION.....	36

2.3.1	<i>Empirical formulae</i>	36
2.3.2	<i>Theoretical formula</i>	40
2.3.3	<i>Modified Kozeny formulae</i>	45
2.3.4	<i>Idealized permeable media</i>	52
2.3.5	<i>Customized models</i>	54
2.4	THE EFFECTS OF CHEMICAL REACTION IN FRACTURED MEDIA	55
2.4.1	<i>Parallel fractures model</i>	56
2.4.2	<i>Idealized fracture model</i>	59
2.4.3	<i>Empirical model</i>	60
2.5	PRESSURE DEPENDENT POROSITY AND PERMEABILITY	61
2.6	REACTION SURFACE AREA	63
2.7	INSTABILITY AND CONCENTRATION DEPENDENT PROPERTIES	67
2.7.1	<i>Concentration dependent permeability</i>	68
2.7.2	<i>Concentration dependent viscosity</i>	69
2.8	CONCLUSIONS	70

CHAPTER 3: DIFFUSION AND DISPERSION IN POROUS MEDIA ...
 **73**

3.1	INTRODUCTION	73
3.2	MOLECULAR DIFFUSION IN POROUS MEDIA.....	74
3.2.1	<i>Bulk diffusion</i>	75
3.2.2	<i>Diffusion in periodic matrix</i>	80
3.2.3	<i>Knudsen diffusion (gas diffusion at low pressure)</i>	81
3.2.4	<i>Surface diffusion</i>	82
3.3	DISPERSION IN POROUS MEDIA	83
3.4	MULTI-COMPONENT DIFFUSION IN POROUS MEDIA.....	85
3.5	DIFFUSION/DISPERSION IN TOUGH2	86
3.6	DIFFUSION AND REACTION CONTROLLED CHEMICAL REACTIONS	91
3.7	CONCLUSIONS	92

CHAPTER 4: NUMERICAL METHODS AND TEST PROBLEMS .. 94

4.1	INTRODUCTION	94
-----	--------------------	----

4.2	THERMAL DIFFUSION WITH HEAT SOURCE (TEST PROBLEM-1).....	97
4.2.1	<i>Test problem-1a (2-D)</i>	97
4.2.2	<i>Test problem-1b (2-D)</i>	101
4.3	REACTION-DIFFUSION (TEST PROBLEM-2).....	107
4.3.1	<i>Test problem-2a (1-D)</i>	107
4.3.2	<i>Test problem-2b (2-D)</i>	112
4.3.3	<i>Test problem-2c (1-D)</i>	115
4.3.4	<i>Test problem-2d (2-D)</i>	120
4.3.5	<i>Reaction-diffusion with Arrhenius reaction rate (Test problem-3)</i>	122
4.4	ADVECTION-DIFFUSION-REACTION (TEST PROBLEM-4)	128
4.4.1	<i>Test problem-4a</i>	128
4.4.2	<i>Advection-Dispersion (problem-4b)</i>	131
4.5	NUMERICAL STIFFNESS (TOUGH2 TEST)	133
4.6	NUMERICAL DISPERSION	138
4.7	CONCLUSIONS.....	141

CHAPTER 5: SPONTANEOUS HEATING OF COAL AND THE

DIMINISHING REACTION RATE..... 141

5.1	INTRODUCTION	141
5.2	THE MAIN FACTORS AFFECTING SPONTANEOUS HEATING OF COAL.....	142
5.2.1	<i>Coal rank</i>	142
5.2.2	<i>Moisture content</i>	143
5.2.3	<i>Temperature</i>	144
5.2.4	<i>Previous Oxidation (aging effect)</i>	145
5.2.5	<i>Oxygen supply</i>	145
5.2.6	<i>Particle size</i>	146
5.2.7	<i>Mineral content (ash and volatile content)</i>	147
5.3	MATHEMATICAL MODELLING OF SELF-HEATING	148
5.3.1	APPROXIMATION OF THE ARRHENIUS TERM.....	153
5.4	REACTANT CONSUMPTION	154
5.5	DIMINISHING REACTION RATE.....	156
5.5.1	<i>Diminishing reaction rate model</i>	157
5.5.2	<i>Previous diminishing reaction models</i>	161

5.5.3	<i>Modified diminishing reaction theory</i>	165
5.5.4	<i>Temperature equation</i>	171
5.5.5	<i>Non-isothermal version of the corrected Chen and Wake model</i>	176
5.5.6	<i>Non-isothermal version of the time dependent model</i>	179
5.5.7	<i>Non-diminishing reaction</i>	182
5.5.8	<i>Elovich model</i>	183
5.6	COMPARISON OF RESULTS AND CONCLUSIONS	184

CHAPTER 6: MODELLING SPONTANEOUS COMBUSTION OF COAL: THE ADIABATIC TESTING PROCEDURE 190

6.1	INTRODUCTION	190
6.2	THE ADIABATIC TESTING PROCEDURE	191
6.3	THE GOVERNING EQUATIONS: TOUGH2 FORMULATION	196
6.3.1	<i>Reaction models</i>	202
6.3.2	<i>Thermodynamic properties of gases</i>	208
6.3.3	<i>Physical properties of coal</i>	213
6.4	MODELLING PROCEDURE	215
6.5	MODELLING RESULTS	216
6.6	CONCLUSIONS.....	226
6.7	POSSIBLE FUTURE WORK.....	227

CHAPTER 7: MODELLING SPONTANEOUS COMBUSTION OF MOIST COAL..... 228

7.1	INTRODUCTION	228
7.2	MODELLING MOISTURE EFFECTS.....	231
7.3	THE GOVERNING EQUATIONS: TOUGH2 FORMULATION	237
7.3.1	<i>Thermodynamic properties of gases</i>	245
7.3.2	<i>Transport properties of wet coal piles</i>	249
7.3.3	<i>Reaction models</i>	251
7.4	MODELLING PROCEDURE.....	252
7.5	MODELLING RESULTS.....	253
7.5.1	<i>Reaction with no moisture enhancement</i>	253

7.5.2	<i>Reaction with moisture enhancement</i>	256
7.5.3	<i>Permeability effects</i>	262
7.5.4	<i>Porosity effects</i>	264
7.5.5	<i>Adiabatic (no flow) Boundaries</i>	267
7.5.6	<i>Reaction and real air</i>	269
7.6	CONCLUSIONS	270
7.7	FUTURE WORK	272

CHAPTER 8: MODELLING COALBED METHANE RESERVOIRS ...

	274
8.1	INTRODUCTION	274
8.2	MAIN FEATURES OF COALBED METHANE RESERVOIRS.....	276
8.2.1	<i>Adsorption and desorption (sorption) of methane</i>	277
8.2.2	<i>Permeability</i>	288
8.2.3	<i>Relative permeability</i>	295
8.2.4	<i>Water Saturation</i>	299
8.2.5	<i>Salinity</i>	301
8.2.6	<i>Capillary pressure</i>	301
8.2.7	<i>Gas Diffusion</i>	302
8.3	MODELLING CBM RESERVOIR	303
8.3.1	<i>TOUGH2 Procedure</i>	307
8.3.2	<i>COMET Procedure</i>	308
8.4	EOS11 (WATER, CH ₄).....	313
8.4.1	<i>Thermodynamic properties of a methane/water mixture</i>	318
8.5	SIMPLE TEST OF EOS11	326
8.6	SENSITIVITY STUDIES IN CBM RESERVOIRS	330
8.6.1	<i>Introduction</i>	330
8.6.2	<i>Model Geometry</i>	331
8.6.3	<i>Relative Permeability</i>	333
8.6.4	<i>Fracture half length and skin factor</i>	337
8.6.5	<i>Modelling Approaches</i>	339
8.6.6	<i>Single porosity model</i>	340
8.6.7	<i>Dual porosity model</i>	341

8.7 SUMMARY AND CONCLUSIONS.....357
8.8 FUTURE WORK358

CHAPTER 9: SUMMARY, CONCLUSIONS AND FUTURE WORK

..... **360**

9.1 MAJOR CONTRIBUTIONS.....360
9.2 OTHER CONTRIBUTIONS363
9.3 FUTURE WORK364

APPENDICES

APPENDIX A367
APPENDIX B369
APPENDIX C374
APPENDIX D378
APPENDIX E382
APPENDIX F389
APPENDIX G395

REFERENCES..... 400

List of Figures

CHAPTER 1: CHEMICAL REACTION IN POROUS MEDIA 1

<i>Figure 1-1: Kinetic solution to Robertson (1966) problem of Equation (1.11).....</i>	<i>9</i>
<i>Figure 1-2: Mixed equilibrium-kinetic solution of Robertson (1966) problem</i>	<i>14</i>
<i>Figure 1-3: Numerical solution to Bjurel stiff problem from Enright and Hull, (1976).....</i>	<i>23</i>

CHAPTER 2: THE EFFECT OF CHEMICAL REACTIONS ON THE TRANSPORT PROPERTIES OF POROUS MEDIA .. 26

<i>Figure 2-1: The effect of tortosity in a porous medium showing the straight length and the effective length.</i>	<i>29</i>
<i>Figure 2-2: Permeability versus porosity for different consolidated and unconsolidated clean and shaly sandstone. Data from Pape et al. (2000)</i>	<i>46</i>
<i>Figure 2-3: Comparison between the models of Table 2-2 for $k_o = 1.0$ (Darcy) and different initial porosity values (a) $\phi_o = 0.1$ (b) $\phi_o = 0.5$.....</i>	<i>51</i>
<i>Figure 2-4: Idealized models of permeable media (a) and (b) represent straight capillary models, (c) and (d) are series models. Taken from Verma and Pruess (1988).....</i>	<i>53</i>
<i>Figure 2-5: Schematic diagram for a single set of parallel fracture from Steefel and Lasaga (1994)</i>	<i>56</i>
<i>Figure 2.6: Permeability versus porosity for different fracture apertures ($\delta = 0.001, 0.002, 0.005, 0.01$ and 0.02)......</i>	<i>58</i>

CHAPTER 3: DIFFUSION AND DISPERSION IN POROUS MEDIA 73

<i>Figure 3-1: Diffusion through a spatially periodic packing of spheres.</i>	<i>80</i>
--	-----------

CHAPTER 4: NUMERICAL METHODS AND TEST PROBLEMS .. 94

<i>Figure 4-1: 2-D and 3-D visualization of the initial conditions.....</i>	<i>99</i>
<i>Figure 4-2: Analytical results for test problem-1a.....</i>	<i>99</i>

Figure 4-3: Numerical solution for test problem-1a.....	100
Figure 4-4: Runge-Kutta-Chebyshev results at the upper right hand quarter for Equation (4.5), from Trompert and Verwer (1991).....	104
Figure 4-5: Newton-Raphson results for Equation (4.5) using the standard finite difference technique....	105
Figure 4-6: TOUGH2 simulation results at different time steps for test problem-1b	106
Figure 4-7: Initial conditions for test problem-2a (Temperature and Concentration) with time dependent boundary conditions.	109
Figure 4-8: Analytical results (Equations 4.11 and 4.12) for 1-D reaction-diffusion model (Test problem-2a) with time dependent boundary conditions.	110
Figure 4-9: Numerical results for the 1-D reaction-diffusion model (Test problem-2a) with time dependent boundary conditions	112
Figure 4-10: Initial conditions for quasi two-dimensional reaction-diffusion (Test problem-2b)	113
Figure 4-11: Analytical solution to quasi two-dimensional reaction-diffusion (Test problem-2b)	114
Figure 4-12: Numerical solution to the quasi two-dimensional reaction-diffusion (Test problem-2b).....	115
Figure 4-13: Initial conditions for test problem 2c (adiabatic boundary conditions).....	117
Figure 4-14: Analytical results for one-dimensional reaction-diffusion model (Test problem-2c) with adiabatic boundary conditions	118
Figure 4-15: TOUGH2 results for the one-dimensional reaction-diffusion model (Test problem-2c) with adiabatic boundary conditions	119
Figure 4-16: Initial conditions for 2-D reaction-diffusion with adiabatic boundary.....	120
Figure 4-17: Comparison between analytical and numerical solutions for the temperature distribution after 5 sec.	121
Figure 4-18: Comparison between analytical and numerical solutions for the temperature distribution after 5 sec for a cross section at $y = 0.5$ m through the geometric center.....	121
Figure 4-19: Comparison between analytical and numerical solutions for transient (a) concentration and (b) temperature at $x = 0$ and $y = 0$	122
Figure 4-20: TOUGH2 steady state results for Oxygen and Temperature distribution with ($n = 8$).....	125
Figure 4-21: TOUGH2 steady state results for Oxygen and Temperature distribution with ($n = 13.4$).....	125
Figure 4-22: Gong's (2000) results (blue line) showing (a) Temperature distribution and (b) Oxygen concentration (kg / m^3) distribution with ($n=8$).....	126
Figure 4-23: Gong's (2000) results (green line) showing (a) Temperature distribution and (b) Oxygen concentration (kg / m^3) distribution with ($n=13.4$)	127
Figure 4-24: Comparison between analytical and numerical (TOUGH2) solutions for the concentration distribution of radioactive tracer after 20 days, test problem-4a.	131
Figure 4-25: Steady state comparison between analytical and numerical (TOUGH2) solution for Advection-Dispersion model, from Steefel and MacQuarrie (1996).	133

Figure 4-26: MATLAB results for both (a) non-stiff (b) stiff and mildly stiff solvers for the modified Robertson problem ($\lambda_1 = 400.0$, $\lambda_2 = 3.0$ and $\lambda_3 = 10^4$).136

Figure 4-27: TOUGH2 results for Fully Implicit and Crank-Nicholson Newton-Raphson solvers for the modified Robertson problem ($\lambda_1 = 400.0$, $\lambda_2 = 3.0$ and $\lambda_3 = 10^4$).137

Figure 4-28: Comparison between Fully Implicit, Crank-Nicholson Newton-Raphson and a stiff solvers for the modified Robertson problem, showing the decay of species A and the production of intermediate species B.137

CHAPTER 5: SPONTANEOUS HEATING OF COAL AND THE DIMINISHING REACTION RATE..... 141

Figure 5-1: Temperature versus time for $\delta_0 = 1$. Comparison of the results from the original version of the Chen and Wake model, the original time dependent model, the power law model and the constant rate model..... 186

Figure 5-2: Temperature versus time for $\delta_0 = 1$. Comparison of the results from the corrected version of the Chen and Wake model, the corrected time dependent model, the power law model and the constant rate model..... 186

Figure 5-3: Temperature versus time for three values of δ_0 . Power law model 187

CHAPTER 6: MODELLING SPONTANEOUS COMBUSTION OF COAL: THE ADIABATIC TESTING PROCEDURE 190

Figure 6-1: Diagram of the adiabatic reaction flask (from Beamish et al. (2000) modified from Humphreys et al. (1981)..... 195

Figure 6-2: Bi-linear fit of the data for sample BH35B.196

Figure 6-3: Enthalpy versus temperature for Nitrogen, Oxygen and Carbon dioxide.....211

Figure 6-4: Self-heating profiles for Kopako (New Zealand) coal sample 61/814. Tests were carried out on (12/5/98) and after aging on (7/7/98). The oxygen flow rate was 50 ml / min . Model A includes oxygen consumption in the heat of reaction and Model B has no oxygen consumption in the heat of reaction.219

Figure 6-5: Self-heating profiles for New Vale coal (New Zealand) sample 58/106, tested on (19/5/98). The oxygen flow rate was 50 ml / min . Model A includes oxygen consumption in the heat of reaction and Model B has no oxygen consumption in the heat of reaction.220

Figure 6-6: Self-heating profile for BBL coal (New Zealand) sample 61/810, tested on (14/5/98). The oxygen flow rate was 50 ml / min . Model A includes oxygen consumption in the heat of reaction and Model B has no oxygen consumption in the heat of reaction.220

Figure 6-7: Self-heating profile for Callide coal (Australia) sample BH35F, tested on (30/11/01). The oxygen flow rate was 25 ml / min . Model A includes oxygen consumption in the heat of reaction and Model B has no oxygen consumption in the heat of reaction.221

Figure 6-8: Self-heating profile for Callide coal (Australia) sample BH35B, tested on (27/11/01). The oxygen flow rate was 50 ml / min . Model A includes oxygen consumption in the heat of reaction and Model B has no oxygen consumption in the heat of reaction.221

Figure 6-9: Self-heating profile for Callide coal (Australia) sample BH35E, tested on (29/11/01). The oxygen flow rate was 100 ml / min . Simulation results are shown for Models A and B using both single (linear) and dual (bi-linear) Arrhenius parameters.222

Figure 6-10: Single straight-line fit to the BH35E coal sample data. Arrhenius parameters $A_0'' = 5.52 \text{ s}^{-1}$ and $E_a = 50.4 \text{ kJ / mol}$ 222

Figure 6-11: Model A simulation results showing temperatures for a test of Callide coal (Australia) sample BH35B. Variable oxygen flow rate.223

Figure 6-12: Model A simulation results showing gas fractions for a test of Callide coal (Australia) sample BH35B. Oxygen flow rate was 50 ml / min223

Figure 6-13: Model A simulation results showing gas fractions for a test of Callide coal (Australia) sample BH35B. Oxygen flow rate was 1 ml / min224

Figure 6-14: Self-heating profile for Callide coal (Australia) sample BH35F (oxygen flow rate of 25 ml / min), studying the effects of changing the coal sample porosity. Simulation results are shown for Model A.224

Figure 6-15: Contours for (a) temperature, (b) oxygen mass fraction, (c) nitrogen mass fraction and (d) carbon dioxide mass fraction for sample BH35B after 763 seconds with oxygen flow rate of 50 ml / min . The left-hand side of each figure is the centerline.225

CHAPTER 7: MODELLING SPONTANEOUS COMBUSTION OF MOIST COAL..... 228

Figure 7-1: The specific enthalpy of air based on the sum of its main components N_2 , O_2 , CO_2 and Ar248

Figure 7-2: The specific enthalpy of air based on data form Felder and Rousseau (1986).....249

Figure 7-3: Linear relative permeability function used in this work251

Figure 7-4: Contours for (a) temperature (b) gas saturation (c) pressure distribution and (d) gas density, for coal with no moisture enhancement of the reaction (see Figure 7-5).254

Figure 7-5: Contours for (a) oxygen mass fraction (b) carbon dioxide mass fraction (c) oxygen mass flow rate (d) Carbon dioxide mass flow rate, for coal with no moisture enhancement of the reaction. Initial saturation $S_v = 0.85$. Time = 2.03 years.255

Figure 7-6: Contours for (a) temperature (b) gas saturation (c) pressure distribution and (d) gas density, for coal with Gong's (2000) moisture enhanced reaction. Initial saturation $S_v = 0.85$ 257

Figure 7-7: Contours for (a) oxygen mass fraction (b) carbon dioxide mass fraction (c) oxygen mass flow rate (d) Carbon dioxide mass flow rate, for coal with Gong's (2000) moisture enhanced reaction. Initial saturation $S_v = 0.85$. Time = 1.35 years.258

Figure 7-8: Temperature cross section profiles of wet-air wet-coal case for model with and without moisture enhancement of the reaction.260

Figure 7-9: The effect of changes in vapour saturation at the center of the model for the standard reaction model (a) temperature versus time (b) gas saturation versus time.260

Figure 7-10: The effect of changes in vapour saturation at the center of the model for the moisture enhanced reaction case. (a) temperature versus time (b) gas saturation versus time.261

Figure 7-11: The effect of changes in permeability on temperature and saturation at the geometric central point for the moisture enhanced reaction model (a) temperature versus time (b) gas saturation versus time.263

Figure 7-12: The effect of changes in permeability on temperature and saturation at the FHZ for the moisture enhanced reaction model (a) temperature versus time (b) gas saturation versus time...264

Figure 7-13: The effect of changes in porosity on behavior at the geometric center (a) temperature versus time (b) gas saturation versus time.266

Figure 7-14: The effect of changes in porosity on behavior at the FHZ (a) temperature versus time (b) gas saturation versus time.266

Figure 7-15: The effect of adiabatic boundary conditions with Gong's (2000) wet reaction term (a) temperature and gas saturation versus time (b) mass fraction of oxygen and carbon dioxide versus time (c) total pressure versus time (d) gas density versus time.....268

Figure 7-16: Four component air with Gong's moisture enhanced reaction model for different gas saturations at the geometric center (a) temperature versus time (b) gas saturation versus time.270

CHAPTER 8: MODELLING COALBED METHANE RESERVOIRS 274

Figure 8-1: Adsorption isotherms of CO_2 and CH_4 (44.5 °C and 1.7 % moisture) for data from Harpalani and Pariti (1993).	284
Figure 8-2: Mass of gas (CO_2 and CH_4) at STP stored per mass of coal versus pressure	286
Figure 8-3: Structure of CBM in coal formation and its flow pattern (from Nugroho and Arsegianto, 1993).	289
Figure 8-4: Relative permeability of gas and liquid according to Equations (8.30) and (8.31) with $k_g^r = 0.9$ and $S_{il} = 0.01$, using Brooks and Corey (1966).	297
Figure 8-5: Comparison between different relative permeability functions for $S_{il} = 0.3$.	298
Figure 8-6: Fracture/matrix model in COMET.	310
Figure 8-7: Comparison between different Henry's law coefficients for dissolution of CH_4 in water.	316
Figure 8-8: Comparison between Henry's law coefficient of CH_4 and CO_2 , calculated using Harvey's (1996) correlation.	317
Figure 8-9: Mass fraction of dissolved in water versus temperature. Based on Harvey's (1996) correlation. Partial pressure of 100 bar.	318
Figure 8-10: Specific enthalpy for CH_4 in the gas-phase.	322
Figure 8-11: Dynamic viscosity for CH_4 in the gas-phase.	324
Figure 8-12: Compressibility factor versus pressure for CH_4 at different temperatures using Pitzer's correlation (from Smith et al., 2001).	326
Figure 8-13: Comparison between CH_4 and CO_2 water systems, for flow in 1D horizontal column.	329
Figure 8-14: Computational grid for a quadrant of the region of interest. 320 acre well spacing and 300 ft fracture half-length, Paul and Young (1993).	333
Figure 8-15: (a) Gas water relative permeability curves for case 112-73, (b) gas water relative permeability curves for Ceder Hill model and laboratory measured curves for the Hamilton No. 3 well, Paul and Young (1993).	335
Figure 8-16: Skin zone around a wellbore, from Croucher et al. (2001b).	338
Figure 8-17: Simulated results for gas production from Area 2 using (a) TOUGH2 (b) COMET, showing the effect of variations in permeability.	345
Figure 8-18: Simulated results for cumulative gas production from Area 2 using (a) TOUGH2 (b) COMET, showing the effects of variations in permeability. Symbols are the same as Figure 8-17.	346
Figure 8-19: Simulated results for water production from Area 2 using (a) TOUGH2 (b) COMET, showing the effects of variations in permeability.	347

Figure 8-20: Simulated results for gas production from Area 1 using (a) TOUGH2 (b) COMET, showing the effects of variations in gas-water relative permeability functions.348

Figure 8-21: Simulated results for cumulative gas production from Area 1 (a) TOUGH2 (b) COMET, showing the effects of variations in gas-water relative permeability functions.349

Figure 8-22: Simulated results for gas production from Area 1 using (a) TOUGH2 (b) COMET, showing the effects of variations in Langmuir volume.350

Figure 8-23: Simulated results for cumulative gas production from Area 1 using (a) TOUGH2 (b) COMET, showing the effects of variations in Langmuir volume.351

Figure 8-24: Simulated results for gas production from Area 1 using (a) TOUGH2 (b) COMET, showing the effects of variations in desorption pressure.352

Figure 8-25: Simulated results for cumulative gas production from Area 1 using (a) TOUGH2 (b) COMET, showing the effects of variations in desorption pressure.353

Figure 8-26: Idealized double porosity model for fractured porous media from Pruess et al. (1999)354

Figure 8-27: Simulation results for gas production rate from Area 1 using TOUGH2-dual porosity model, showing the effects of variations in fracture permeability.354

Figure 8-28: Simulation results for the cumulative gas production from Area 1 using TOUGH2-dual porosity model, showing the effects of variations in fracture permeability.355

Figure 8-29: Simulation results for the cumulative gas production from Area 1 using TOUGH2-dual porosity model, showing the effects of variations in matrix permeability.355

Figure 8-30: Simulation results for the cumulative gas production rate from Area 1 using TOUGH2-dual porosity model, showing the effects of variations in methane diffusion coefficient.356

Figure 8-31: Simulation results for the cumulative gas production from Area 1 using TOUGH2 dual porosity model, showing the effects of variations in methane diffusion coefficient.356

Figure 8-32: Simulation results for the cumulative gas production from Area 1 using TOUGH2- dual porosity model, showing the effects of variations in matrix/fracture porosity for two methane diffusion coefficients.357

List of Tables

CHAPTER 2: THE EFFECT OF CHEMICAL REACTIONS ON THE TRANSPORT PROPERTIES OF POROUS MEDIA .. 26

<i>Table 2-1: Different versions of Kozeny's equation</i>	45
<i>Table 2-2: Porosity-dependent permeability based on Kozeny models and their uses</i>	49
<i>Table 2-3: Concentration-dependent permeability relationships</i>	69

CHAPTER 4: NUMERICAL METHODS AND TEST PROBLEMS .. 94

<i>Table 4-1: Summary of the test problems discussed in this chapter</i>	96
<i>Table 4-2: Parameters used in test problem-1a</i>	98
<i>Table 4-3: Solution parameters for test problem-1b, from Trompert and Verwer (1991)</i>	101
<i>Table 4-4: Parameters used in test problem-2a</i>	109
<i>Table 4-5: Parameters used in test problem-2c</i>	116
<i>Table 4-6: Coal parameters for dry coal for test problem-3, from Gong (2000)</i>	124
<i>Table 4-7: Parameters for Radioactive tracer test problem-4a, from Oldenburg and Pruess (1995)</i>	130
<i>Table 4-8: Data for test problem-4b from Steefel and MacQuarrie (1996)</i>	132

CHAPTER 5: SPONTANEOUS HEATING OF COAL AND THE DIMINISHING REACTION RATE..... 141

<i>Table 5-1: Comparison between Models. Special case $\beta=1$</i>	188
<i>Table 5-2: Comparison between Models. General β</i>	189

CHAPTER 6: MODELLING SPONTANEOUS COMBUSTION OF COAL: THE ADIABATIC TESTING PROCEDURE 190

<i>Table 6-1: Polynomial coefficients for specific heat capacity of gases N_2, O_2 and CO_2 from Felder and Rousseau (1986)</i>	210
<i>Table 6-2: Approximate densities for the main components of coal</i>	213

Table 6-3: Experimental data for New Zealand and Australian coal samples.....214

**CHAPTER 7: MODELLING SPONTANEOUS COMBUSTION OF
MOIST COAL..... 228**

Table 7-1: Parameter value list from Gong (2000).....236
Table 7-2: Constant values from Gong (2000).....236
Table 7-3: Harvey's correlation coefficients, (Harvey, 1996).....246

CHAPTER 8: MODELLING COALBED METHANE RESERVOIRS274

Table 8-1: Polynomial coefficients for Henry's law, from Cramer (1982)314
Table 8-2: Coefficients for Henry's law, from Harvey (1996)315
Table 8-3: Polynomial coefficients for Equation (8-62) from Felder and Rousseau (1983).....321
Table 8-4: Coefficients for Equation (8.64), from Battistelli et. al. (1997).321
Table 8-5: Coefficients for dynamic viscosity of equation (8.67), from Irvine and Liley (1984).....324
Table 8-6: Tube model data used for CH_4 and CO_2 compression test328
Table 8-7: Standard data used for the sensitivity study from Paul and Young (1993).336
Table 8-8: Conversion from customary to metric units.337

Nomenclature

Because of the extensive literature review and the many different applications discussed in this work, it is impossible to have a common notation throughout the thesis. The nomenclature given below includes the notation used throughout the work, while the other notation is defined differently as it appears in each chapter.

A	Area	m^2
A_0	Arrhenius pre-exponential factor (first order)	$1/s$
A'_0	Arrhenius pre-exponential factor for coal (Chapter 6)	$m^3/kg_{coal} s$
A''_0	Arrhenius pre-exponential factor (zero order)	$1/s$
Bi	Biot number $Bi = hx/K$	
C	Concentration	kg / m^3
C_p	Specific heat capacity	kJ / kgK
c_K	Cozeny's constant	
c	Compressibility	$1 / Pa$
D	Diffusion coefficient	m^2 / s
D_{th}	Thermal diffusivity $D_{th} = K / \rho C_p$	m^2 / s
$d_{\beta}^{(\kappa)}$	Diffusion coefficient of phase β in component κ	m^2 / s
d	Diameter	m
E_a	Activation energy	J / mol
F_f	Formation factor (Chapter 3)	
$\mathbf{F}^{(\kappa)}$	Flux of component κ	$kg / m^2 s$ or $J / m^2 s$
$f^{(\kappa)}$	Mass fraction of component κ adsorbed per mass of solid	kg^{κ} / kg^{solid}

g	Gravitational acceleration	m / s^2
$G_s^{(i)}$	Gas storage capacity of component i	m^3 / kg_{coal}
h	Heat transfer coefficient (convection)	$W / m^2 K$
h	Cleat thickness (Chapter 8)	m
$H^{(\kappa)}$	Enthalpy of component κ	J / kg
h_{fg}	Latent heat of water	J / kg
J	Jacobian matrix	
K	Thermal conductivity	$W / m K$
k	Permeability	$m^2 (10^{-12} \text{ Darcy})$
K_d	Distribution coefficient	m^3 / kg_{solid}
K_h	Henry's constant	$Pa (N / m^2)$
L	Length	m
L_e	Effective length	m
$M_\beta^{(\kappa)}$	Mass accumulation term of component κ in phase β	kg / m^3
M^{NK+1}	Heat accumulation term in multi-phase system	J / m^3
MAD	Adsorbed mass accumulation term	kg / m^3
$MW^{(\kappa)}$	Molar weight of component κ	$kg / kmol$
n	Reaction order	
n	Unit normal vector	
NK	Number of mass components	
NPH	Number of phases	
O_{ad}	Oxygen adsorbed on the coal surface	kg_{O_2} / kg_{coal}
$P^{(\kappa)}$	Partial pressure of component κ	$Pa (N / m^2)$
P	Pressure	$Pa (N / m^2)$
Q	Ionic activity product (Chapter 1)	
Q	Heat released by reaction (Exothermicity)	J / kg

$q^{(\kappa)}$	External sink/source of component κ	$kg / m^3 s$ or $J / m^3 s$
R	The universal gas constant (8.3145)	$kJ / kmol K$
R_t	Retardation factor (Chapter 4 and Chapter 8)	
Rf	Recovery factor (Chapter 8)	
R_{70}	Self-heating rate index (40 to 70 °C) (Chapter 6)	$^{\circ}C / hour$
RH	Relative Humidity	
r	Radius	m
$r^{(\kappa)}$	Reaction rate of component κ	$kg / m^3 s$
Re	Reynolds number	
S	Saturation	
SR	Stiffness ratio	
T	Temperature	$^{\circ}C$
T_K	Absolute Temperature	K
t	Time	$s (sec)$
t_{pr}	Prior reaction (oxidation) time (Chapter 5)	$s (sec)$
U	The intrinsic velocity	m / s
u	Specific internal energy	J / kg
V	Darcy's velocity (volume flux) ($V = \phi.U$)	m / s
V_n	Volume of grid element n	m^3
$X_{\beta}^{(\kappa)}$	Mass fraction of component κ in phase β	$kg_{\beta}^{(\kappa)} / kg_{\beta}^{(total)}$
x	Distance	m
$Z^{(\kappa)}$	Compressibility factor of component κ	
Γ_n	Surface area of grid element n	m^2
Γ	Gama function (Chapter 5)	
α	Molar weight ratio	
α	Empirical constant for the diminishing rate law (Chapter 5)	
α_L	Longitudinal dispersion coefficient	m^2 / s

α_T	Transverse dispersion coefficient	m^2 / s
∇	Gradient	
λ	Reaction rate coefficient	
λ	Non-isothermal reaction rate coefficient, $\lambda = A_0 \exp(-E_a/RT)$	
λ_0	Isothermal reaction rate coefficient, $\lambda_0 = A_0 \exp(-E_a/RT_0)$ (Chapter 5)	
ρ	Density	kg / m^3
ν	Kinematic viscosity (μ/ρ)	m^2 / s
μ	Dynamic viscosity	$N s / m^2$ (Pa s)
μ	Constant, $\mu = 1/\delta_0 (1 + \beta)$ (Chapter 5)	
ν	Reaction stoichiometric coefficient	
χ	Mole fraction	
β	Constant $\beta = Q / \rho C_p$ (Chapter 4)	
β	New empirical constant for the diminishing rate law (Chapter 5)	
δ_0	Modified Frank-Kamenetskii parameter (Chapter 5)	
	$\delta_0 = (E_a / RT_0^2) (Q O_0 A_0 \tau / C_p) \exp(E_a / RT_0)$	
ε	Reduced ambient temperature, $\varepsilon = RT_0 / E_a$ (Chapter 5)	
γ	Incomplete Gamma function (Chapter 5)	
ξ	Constant, $\xi = 1/\nu(1 + b)$ (Chapter 5)	
ν	Constant, $\nu = \sigma/\varepsilon$ (Chapter 5)	
θ	Reduced excess temperature, $\theta = (T - T_0)E_a / RT_0^2$ (Chapter 5)	
σ	Constant, $\sigma = Q O_0 / C_p T_0$ (Chapter 5)	
τ	Tortuosity ($\tau = L_e / L$) $\tau > 1$	
τ	Characteristic time scale ($\tau = t / t_{pr}$) (Chapter 5)	
τ	Sorption time (Chapter 8)	s (sec)
τ_f	Tortuosity factor ($\tau_f = \tau^2$)	
ϕ	Porosity	

Subscripts

<i>ad</i>	Adsorption
<i>b</i>	Bulk
<i>coal</i>	Coal
<i>eff</i>	Effective
<i>eq</i>	Equilibrium
<i>f</i>	Fluid
<i>f</i>	Fracture (Chapter8)
<i>g</i>	Gas
<i>in</i>	Insoluble mineral (Chapter2)
◦	Initial state (initial condition)
<i>L</i>	Langmuir
<i>l</i>	Liquid
<i>m</i>	Mixture
<i>m</i>	Soluble mineral (Chapter2)
<i>m</i>	Matrix (Chapter 8)
<i>p</i>	Particle
<i>r</i>	Relative
<i>s</i>	Solid
<i>s</i>	Skin (Chapter8)
<i>std</i>	Standard conditions (101325 Pa and 288.6 K) (Chapter 8)
<i>v</i>	Vapor
β	Phase (gas or liquid)

Superscript

<i>adv</i>	Advective
<i>air</i>	Air
<i>Ar</i>	Argon
<i>CH₄</i>	Methane
<i>CO₂</i>	Carbon dioxide

<i>dis</i>	Diffusive (dispersive)
<i>e</i>	Equilibrium
N_2	Nitrogen
O_2	Oxygen
<i>sat</i>	Saturation conditions
κ	Component (mass or heat)
*	Non-dimensional form (Chapter5)

Abbreviations

BHP	Bottom hole pressure
CBM	Coalbed methane
DEA	differential-algebraic equations
ECBM	Enhanced coalbed methane
EOS	Equation of state
FHZ	Fastest heating zone
IFDM	Integrated finite difference method
MINC	Multiple interacting continua
NR	Newton-Raphson
ODE	Ordinary differential equation
PDE	Partial-differential equations
REV	Representative elementary volume
STP	Standard temperature and pressure (101325 Pa and 288.6 K)
TDS	Total dissolved solids